Periodica Polytechnica Civil Engineering, 68(1), pp. 232–247, 2024

The Effects of Sequential Aftershocks on the Behavior of the Irregular RC Buildings

Farhad Hosseinlou[1*], Mojtaba Labibzadeh[1]

[1] Faculty of Civil Engineering and Architecture, Shahid Chamran University of Ahvaz, Golestan Blvd., University Square, 6135783151 Ahvaz, Iran
[*] Corresponding author, e-mail: f.hosseinlou@scu.ac.ir

Received: 08 July 2022, Accepted: 09 September 2023, Published online: 02 October 2023

Abstract

Studies show that design codes did not provide a reliable way to consider the effects of successive earthquakes on the behavior of the RC buildings. A lot of research are underway in this field, but the effect of shear wall placement in the regular and irregular structures under the seismic sequences and the imposing the vertical acceleration component to them has not been considered. For this purpose, in this study, the Christchurc earthquakes have been employed to observe the effects of seismic sequences on the location of the shear wall in the regular and irregular 3- and 8-story structures. The studied reinforced concrete structures have a dual system of flexural frames with shear walls. In this study, the designed shear wall with ACI code 318-14 is located in the different openings of structures. To model the frame of the structures of concrete flexural frame with wall, the Ibarra and Krawinkler concentrated joint behavioral model has been considered. The Hazus code is utilized to provide the fragility curves and also to indicate the failures based on the four drift-based performance levels. The IDA analysis is then performed on the models and the results are acquired. The failure index is considered as the maximum drift between the floors of the structures. The IR_3S_MO structure under main earthquakes at the three performance levels (Slight, Moderate, Complete) can withstand 11%, 14% and 88% spectral acceleration more than the IR_3S_LO structure, respectively. This ratio is approximately 10%, 12% and 42% for the IR_3S_RO structure, respectively.

Keywords

probability of failure, incremental dynamic analysis, irregular structures, fragility curves, sequential aftershocks, seismic sequences

1 Introduction

Undoubtedly, earthquakes are one of the most dangerous natural disasters that threaten people's lives. Observations from field investigations have shown that in the areas with high seismicity rates, a structure may be exposed to more than one earthquake in a relatively short period of time. Also, these observations represent that strong ground motions are generally accompanied by aftershocks with large peak ground accelerations. The two main components of sequential ground motions are the mainshock and aftershocks. In recent years, the seismic activity of these two components has caused a lot of damage to buildings. Structural destructions caused by the mainshock can be further aggravated by aftershocks, which can lead to structural failure of the buildings [1, 2]. Current structure seismic design approaches commonly employ the mainshock effects only.

Hereupon, performance of structures under earthquake mainshock-aftershock sequences, should constantly be fully examined. In recent years, researchers have done a lot of research on the effect of seismic sequences on the behavior of structures. But it is clear from a review of past research that extensive studies in this area are still needed. Thus, previous studies on the seismic performance of buildings are reviewed. We can refer to the study of Amadio et al. [3], in which the nonlinear behavior of one-degree-of-freedom systems under multiple earthquakes was investigated and the Park-Ang damage index was utilized to assess the structural damage. Also, Hatzigeorgiou and Liolios [4] studied the nonlinear behavior of reinforced concrete frames under the strong repeated earthquakes. They conducted an extensive study on the nonlinear response of eight reinforced concrete planar frames under forty-five seismic sequences. The results of this study showed that the response and design of reinforced concrete frames are significantly affected by seismic sequences. They also presented a relationship for predicting the ductility demand under the successive earthquakes using a simple combination of the

Cite this article as: Hosseinlou F., Labibzadeh M. "The Effects of Sequential Aftershocks on the Behavior of the Irregular RC Buildings", Periodica Polytechnica Civil Engineering, 68(1), pp. 232–247, 2024. https://doi.org/10.3311/PPci.20795

ductility demand under single earthquakes. Abdelnaby and Elnashai [5] conducted a study to investigate the deterioration of reinforced concrete frames under seismic sequences caused by the Tohoku and Christchurch earthquakes. After these two earthquakes, studies showed that the destruction of structural systems occurred due to multiple earthquakes. The reported damages were mainly due to the loss of stiffness and strength of the structural elements as a result of material deterioration during seismic loading. The models of nonlinear reinforced concrete frames containing failure characteristics were developed and time history analyzes were performed on them. The results showed the significant effect of multiple earthquakes on the behavior of structures.

Moshref et al. [6] developed the methods for accurate modeling of the column behavior under seismic loading. For this purpose, seven shaking table tests were employed to evaluate the accuracy of modeling methods considering residual displacement, maximum displacement, and base shear. It was found that although the recommended modeling methods can estimate the maximum displacement and maximum base shear with reliable accuracy, the difference in their results related to residual deformation is not acceptable. The modified concrete model, which represents the cumulative failure due to the loading cycle, was then applied to the fiber element analysis. Using the modified concrete model, the error of modeling methods (along with residual displacement) was reduced.

Abdelnaby and Elnashai [7] developed a process for numerical analysis of concrete structures subjected to multiple earthquakes and conducted a parametric study on the effects of multiple earthquakes in the response of reinforced concrete frames. For this purpose, the concrete structural models with suitable properties for considering damage were produced utilizing fiber elements. The results showed that the decay of structural systems was effectively affected by the sequence of earthquakes, however, it cannot be predicted by simple analysis. It was also confirmed that the effects of multiple earthquakes on seismic safety are significant. Song et al. [1] provided a framework for estimating the damage of steel structures under seismic sequences. The proposed framework was utilized to investigate the effects of aftershocks on the seismic damages. Monte Carlo simulation and Latin Hypercube sampling were employed to examine the uncertainty in the damage estimation. The results showed that even if the aftershocks had a small effect on the response of the structure, it may had a significant effect on seismic damage because of the existence of uncertainty in the failure condition.

Abdelnaby [8] accomplished a seismic assessment of the fragility relationships for reinforced concrete frame systems under seismic sequences because the destructive effects of aftershocks are ignored by current building codes. The results of this study showed that multiple earthquakes have significant effects on the vulnerability relationships of concrete frames. Wen et al. [9] proposed a method for assessing the vulnerability of structures under seismic sequences. The effects of aftershocks on the fragility of a 5-story reinforced concrete frame were investigated. Hosseinpour and Abdelnaby [10] investigated the fragility curves for concrete frames affected by multiple earthquakes. These studies were done with the aim of overcoming previous limitations and obtaining the fragility curves for 3 reinforced concrete frames with the number of floors 3, 7 and 12 and under multiple earthquakes. Hosseinpour and Abdelnaby [11] presented a paper to examine the important limitations in the recent studies, which are: (a) using the earthquake records caused by unrelated events in different places; (b) using the simple models that do not contain damage tolerance features; (c) lack of attention to the effects of earthquake direction, seismic polarity, aftershock, irregularity in the structure and the vertical component of earthquake. The results showed that the direction of the earthquake in the irregular structure, and the vertical component of the earthquake can have a significant effect on the response of the structure (subjected to multiple earthquakes). The findings also showed that the aftershock polarity can significantly change the response of irregular structures. Rostamian et al. [12] investigated the effect of seismic reinforcement on the behavior of reinforced concrete bridge columns subjected to the seismic sequences of main earthquakes and aftershocks. They examined the nonlinear behavior of FRP-covered columns of the bridge under the multiple earthquake records. The results showed that considering full coverage for the bridge columns can improve structural performance slightly and also the damage caused by the main earthquakes in sequences for a long bridge is negligible. Omranian et al. [13] considered the development of fragility curves to assess the seismic vulnerability of reinforced concrete bridges under the seismic sequence, main earthquake, and aftershock. They examined the seismic damage of an arched bridge under the earthquake sequence. The results showed that the aftershocks had an exponential effect on the vulnerability of bridges. In addition, the retrofitting methods significantly affect the seismic response of bridges and buildings and thus their fragility [14–16]. Oyguc et al. [17] done a study to consider the deterioration

behavior of irregular reinforced concrete structures under the sequence of Tohoku earthquakes. The results showed that the effects of multiple earthquakes are significant, and the effects of irregularity increase the scattered damage under these vibrations. Hamidi Jamnani et al. [18] studied the seismic behavior of structures with concrete shear walls and the structural response and energy distribution of these structures under the individual earthquakes and seismic sequences. The aim of this study was to investigate the seismic sequence records and the energy concepts resulting from their application. The performed analyzes showed that the sequential earthquakes increased the seismic requirements of flexural frames with concrete shear walls.

Amiri and Bojórquez [19] examined the residual displacement ratio of structures as single-degree freedom systems (linear) under the seismic sequences (main earthquake plus one aftershock). Because the residual displacement can determine the residual capacity of damaged structural systems as an effective predictor parameter. Hassan et al. [20] designed three semi-rigid frames with different connection capacities and examined their performance under sequential earthquakes. They examined the seismic performance of the frames for two purposes: (a) the development of fragility functions for structures under seismic sequences and main earthquakes and (b) evaluating the rate of nonlinear expansion and elongation of the period in the structures designed based on sequence events. The results showed that the application of aftershocks increases the probability of overcoming a level of failure in the frames, which is mainly due to the elongation of the period and also existence of the permanent failures. Di Sarno and Wu [21] evaluated the fragility of steel frames. The steel frames had a brick filling wall that are not seismically designed. Evaluating the effect of multiple earthquakes on the cumulative damage of steel frames is an important part of performance earthquake engineering. The effect of brick filler walls on the vulnerability of steel frames has been considered. The fragility curves of aftershocks were extracted and studied to identify the seismic vulnerability of the brick fillers of the frames damaged by the main earthquake. An overview of the mentioned studies shows that so far, no research has been done on the effect of shear wall placement in the concrete frames with concentrated joint behavioral model (Ibarra-Krawinkler) under the effect of seismic sequence. So, the current paper seeks to investigate this issue. In the current paper, the structures presented in the study of Hatzigeorgiou and Liolios [4] will be applied to model the regular and irregular 3 and 8 story reinforced concrete frames. The shear walls are located in different openings of the studied frames. Using the incremental dynamic analysis (IDA) method, the effect of shear wall placement under major New Zealand CHRISTCHURCH earthquakes and their seismic sequences are assessed. Moreover, the Ibarra and Krawinkler concentrated joint behavioral models have been considered to model the frame of dual structures of flexural frames with walls; because this model has the ability to consider the more collapse modes than other models. Obtaining and comparing the occurrence probability diagrams respect to spectral acceleration of the models obtained from the effect of reinforced concrete shear wall placement in the four performance levels is the another desired goal. The four performance levels (Slight, Moderate, Extensive and Complete) mentioned in the Hazus Code [22] are employed.

2 Methodology and modeling

In this research, the regular and irregular 3- and 8-story reinforced concrete frames have been employed. In these structures, the compressive strength of concrete equal to 20 MPa and the yield strength of steel equal to 500 MPa are selected. Dead and live load values are considered to be 20 and 10 kN on the frame beams, respectively. These structures are designed according to the Eurocode 8 [23] and to accelerate the 0.2g (high seismic hazard zone). However, it should be noted that in these models, the shear rebars are not presented in the reference paper [4]; but due to the need for shear rebars, values are considered for them. The shear reinforcements No. 10 (with a distance of 15 cm in the beams and with a distance of 20 cm in the columns) have been considered. For the regular and irregular 3-story reinforced concrete frames, the columns with dimensions of 30 × 30 (cm) and beams with dimensions of 30 × 40 (cm) are utilized. Other specifications include how the rebars are laid and their number are shown in Figs. 1 and 2. For the regular and irregular 8-story reinforced concrete frames, the

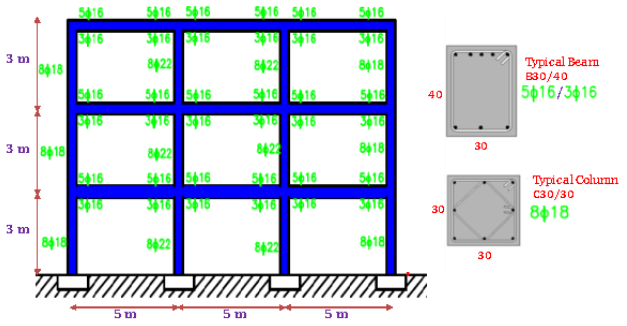

Fig. 1 Regular 3-story frame and its specifications

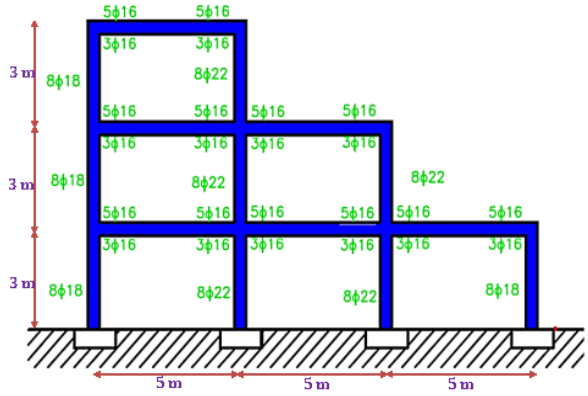

Fig. 2 Irregular 3-story frame and its specifications [4]

columns with dimensions of 40 × 40 (cm), 35 × 35 (cm) and 30 × 30 (cm); and beams with dimensions of 30 × 40 (cm), 30 × 50 (cm) and 30 × 60 (cm) are employed. The specifications of these frames are presented in Figs. 3 and 4. It is worth noting that for the calculations, the mass of the frames is extracted through the ETABS software. The studied frames are also modeled with OpenSees software. Because the IDA analysis is time consuming, a concentrated scheme will be applied to model the frames of this research to reduce the analysis time and to consider the more collapse modes.

In this method, the nonlinear springs are used to indicate the nonlinear performance of structural members. The characteristics of these springs have been acquired using the research of Haselton et al. [24]. Of course, the stiffness adjustment coefficient for beam and column springs is $n = 10$ [25]. Utilizing the "ZeroLength" element, the rotating spring element is introduced, and the two horizontal and vertical transition directions are closed employing the "equalDOF" command. In order to better see the slip effect of the rebar in the cross-sectional connection, a "rigid elastic" element is assigned. The element "Elastic Beam Column" is considered to introduce the beams and columns,

and the springs are placed at both ends of these elements. To consider the effect of the axial load on the rotating spring's moment at the end of the columns, the yield moment relationship presented in the Telemachos and Fardis [26] is implemented. For the present study, a shear wall are designed considering the frame opening width of 3 m. The ACI 318-14 code have been applied to design the shear walls [27]. Table 1 shows the specifications of the rebars used in these walls. In this work, two modeling methods are considered to model and introduce reinforced concrete shear walls.

For shear walls where the ratio of height to width is less than or equal to 2($H/l \leq 2$), the wall is of Squat type and the behavior of the wall will be the shear behavior. When

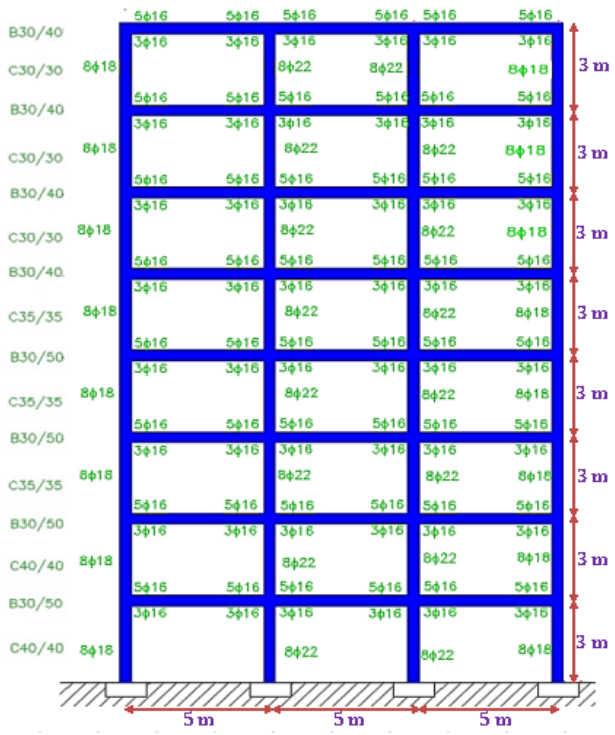

Fig. 3 Regular 8-story frame and its specifications [4]

Fig. 4 Irregular 8-story frame and its specifications [4]

Table 1 Specifications of shear wall rebars

Rebars	Number	Distance	Reinforcement ratio
Horizontal	12	25 cm	Horizontal
vertical	16	25 cm	vertical

$H/l \leq 2$, the wall is of the slender type and the behavior of the wall will be the bending behavior. In this study, for $H/l \leq 2$, the wall is modeled utilizing a shear spring at a height of elements, and the flexural (bending) behavior of the wall is avoided. To introduce this spring, "uniaxialMaterial Hysteretic" is employed in OpenSees software. In this regard, the shear behavior presented in FEMA356 have been utilized.

The ASCE/SEI 41 Concrete Provisions provides the updated values for these parameters. In the frames with thick shear walls, the axial force ratio in the walls is almost less than 0.05 [28]. MVLEM element is considered to model the slender walls, and CONCRETE06 and STEEL02 materials are applied to model the concrete and steel elements in the wall, respectively. The results of previous research show that usually each floor is modeled using two MVLEM elements, and 8 elements are employed in the transverse direction so that each has a size between 70 to 90 cm [29]. The shear wall element is attached to the concrete frame via a rigid elastic column beam element, then the shear walls are placed in the openings of the frames. The crack coefficient is considered to be 0.5 for the wall elastic element and 0.4 for the wall shear spring [28]. For more information in this regard, refer to Orakcal et al. [30].

3 Validation of the models

In this section, the validity of the models is presented. As mentioned, the mass of the structure (mass of beams and columns) is obtained via ETABS software. The calculated mass is applied to the structure along with dead load (20 kN/m) and live load (10 kN/m). The uropean regulations consider the composition of the load [100%DL + 25%LL] (Eurocode 8, 2005). In this section, the periods of the proposed models are compared with the periods of the models presented in the study of Hatzigeorgiou and Liolios [4]. The specifications of the frames are presented in Figs. 1 to 4. The validation results based on the periods are listed in Table 2. The results obtained in this validation are in good agreement with the main results of the reference article [4]. In order to show that the modeling performed in the present research is performed correctly, the concrete structures are validated using a time history diagram.

For this purpose, a 5-story reinforced concrete frame with a shear wall presented in the investigation of Kolozvari et al. [29] are employed. This structure is designed based on ASCE 7-10 and ACI 318-11 regulations [27, 31], which will mention some of the model specifications. The specifications of the member cross sections and dimensions are given in Fig. 5 and Table 3. In this model, the beams and columns of the frame are modeled by the concentrated joint method. For each floor, the wall is modeled through two SFI-MVLEM elements. The walls are then fastened to the frame horizontally. The beams and columns are modeled according to the specifications shown in Fig. 5. For beams and columns, an elastic element is considered with two nonlinear springs at both ends. The record of Fig. 6 is selected from the center of PEER NGA with a maximum ground acceleration of 0.3g. By applying it to the studied models, the desired structural responses of both models are achieved.

After modeling and applying the earthquake record, the comparison of the analysis results is shown in Table 4 and Fig. 7. Table 4 shows that the periods obtained from both models are in good agreement, which is acceptable.

Table 2 The validation results based on the periods

Results	Frames	First Mode (s)	Second Mode (s)	Third Mode (s)
Reference Paper	Irregular 3-story	0.5	0.2037	0.1308
	Regular 3-story	0.6382	0.2048	0.1215
	Irregular 8-story	0.9673	0.4469	0.2746
	Regular 8-story	1.2330	0.4718	0.2651
Current Paper	Irregular 3-story	0.4988	0.2157	0.1392
	Regular 3-story	0.6358	0.2154	0.1282
	Irregular 8-story	0.9898	0.4526	0.2893
	Regular 8-story	1.2170	0.4632	0.2706

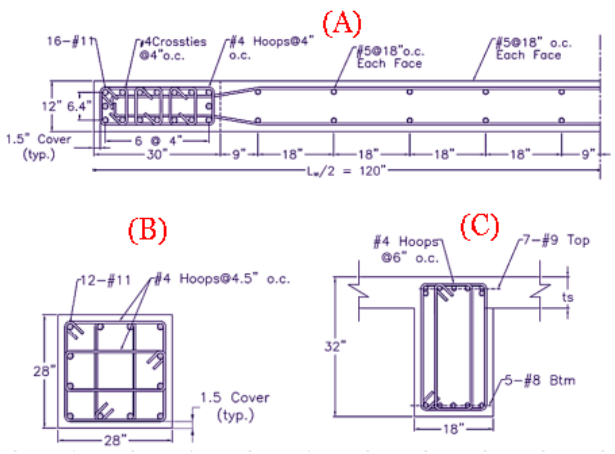

Fig. 5 The specifications of the member cross sections: (A) wall, (B) column, and (C) beam [30]

Table 3 Model details of Kolozvari et al. [29]

Compressive strength	5 ksi	Dimensions of beams	18 × 32 inch
Steel yield strength	60 ksi	Dimensions of columns	12 inch
Dead load	150 psf	Length of wall opening (width)	20 ft
Live load	40 psf	Floor height of the wall	12 ft
The length of the opening	20 ft	Proportion of transverse and longitudinal rebars	0.0025
Floor height	12 ft	Wall thickness	12 inch

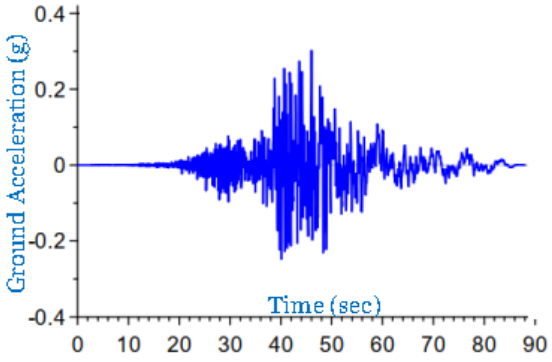

Fig. 6 Acceleration time history applied to frames

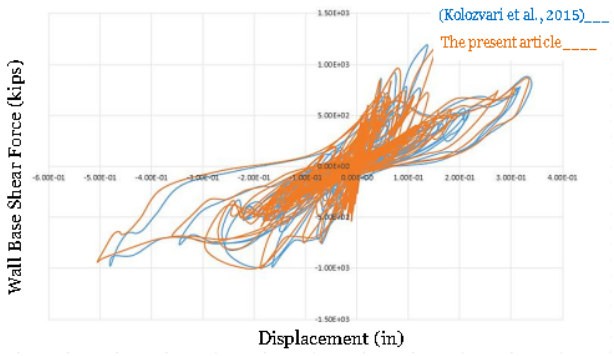

Fig. 7 Validation of two models under the applied record

Table 4 Periods of the simulated model and the base model

Period (Sec)	first mode	second mode
The model of present study	0.533	0.104
The model of Kolozvari et al. (2015)	0.534	0.104

But to further ensure the accuracy of the model, the analysis results of the two structures under the seismic record will be compared. The results will be as shown in Fig. 7. Calculations indicate that for both models, the maximum value of the shear force is equal to 1.3×10^3 *Kips*, and the maximum value of displacement is approximately in the range of 0.35–0.5 *in*. Also, the ductility ratio is 0.76 and the strength ratio is 0.61. The hysteresis curves show that the modeled structure has a close response to the structure of the reference paper [30], so the modeling is done correctly. Modal analysis is performed to indicate the effect of wall placement in these models.

4 Establishment of the final structural frames

After validating the models, the shear walls are located in the various openings of models and then ten models are created. One of the effective ways to ensure the accuracy of modeling is to perform appropriate analyzes so that the behavior of the structure can be determined using the gained results. The results of their analysis will be presented in different sections.

4.1 Wall placement in regular and irregular frames

Fig. 8 shows the regular 8-story reinforced concrete structure with a shear wall in the middle and left openings. The presented shear walls in Fig. 8 are slender walls. Fig. 9 shows three models created by wall placement in the irregular 8-story frame. The presented shear walls in Fig. 9(a,b) are slender and have a bending behavior. But in Fig. 9(c), the used shear wall is a thick or short wall.

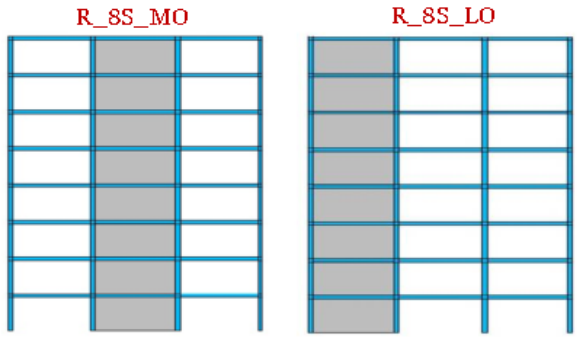

Fig. 8 The regular 8-story reinforced concrete structure (R_8S) with a shear wall in the middle openings (MO) and left openings (LO)

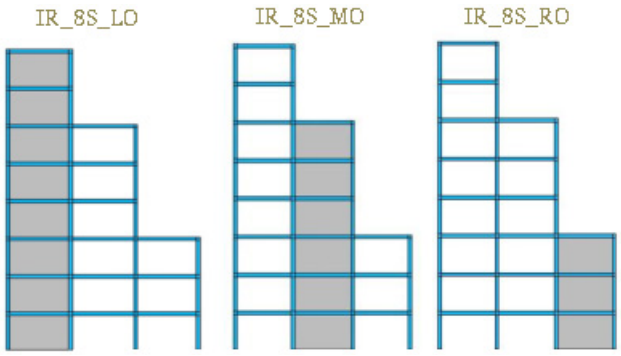

Fig. 9 The irregular 8-story reinforced concrete structure with a shear wall in the (a) left, (b) middle and (c) right openings

Fig. 10 demonstrations the regular 3-story reinforced concrete structure with a shear wall in the middle and left openings. Fig. 11 displays three models produced by wall placement in the irregular 3-story frame. The utilized shear walls in Figs. 10 and 11 are thick or short wall and have a shear behavior. Modal analysis is performed to indicate the effect of wall placement in these models. The periods of each model are calculated through OpenSees software, which is listed in Table 5. The effects of wall placement on the period of validated structures are now being investigated. Table 5 demonstrations that the period of flexural frame structures is significantly reduced by wall placement in them. In other words, with increasing the height of the wall, the stiffness of the whole structure also increases and as a result, the periods are further reduced.

4.2 Pushover analysis of the created models

In this analysis, a monotonic load is applied to the created models at the level of each floor and the roof drift of the structure is considered as the target value. In this research, the pushover analysis is accomplished on each model and its diagram is acquired. The horizontal axis of the diagram is the drift, and the vertical axis is the base shear force. In this research, the pushover analysis is accomplished on each model and its diagram is acquired. The horizontal axis of the diagram is the drift, and the vertical axis is the base shear force. First, the pushover diagrams of the four initial structures (without shear wall) are displayed. In order to show the complete behavior of the modeled structure employing the concentrated joint method, the target drift has been considered. According to Fig. 12, it can be seen that the regular 8-story structure have the least drift until it reached the decay.

After obtaining the capacity curve diagram of the initial models, the diagrams of the models obtained from the wall placement in regular and irregular 3 and 8 story structures are revealed. The target drift is equal to drift at the roof point, which shows the behavior of the models well

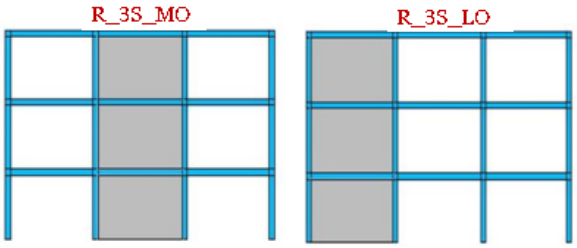

Fig. 10 The regular 3-story reinforced concrete structure with a shear wall in the middle and left openings

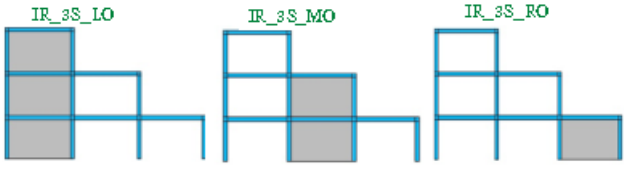

Fig. 11 The irregular 3-story reinforced concrete structure with a shear wall in the (a) left, (b) middle and (c) right openings

Table 5 Comparison of changes in the period of produced frames and primary frames

Validated frames	Periods (Sec)	Produced frames	Periods (Sec)
Regular 3-story	0.4988	R_3S_LO	0.2
		R_3S_MO	0.2
Irregular3-story	0.6358	IR_3S_LO	0.125
		IR_3S_MO	0.22
		IR_3S_RO	0.37
Regular 8-story	0.9898	R_8S_LO	0.42
		R_8S_MO	0.38
Irregular8-story	1.217	IR_8S_LO	0.31
		IR_8S_MO	0.415
		IR_8S_RO	0.77

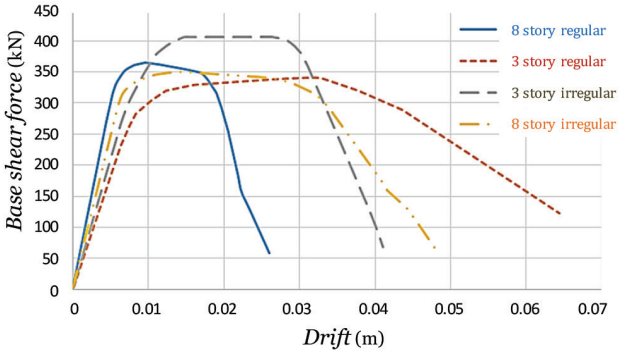

Fig. 12 The pushover curves of the four initial structures (without shear wall)

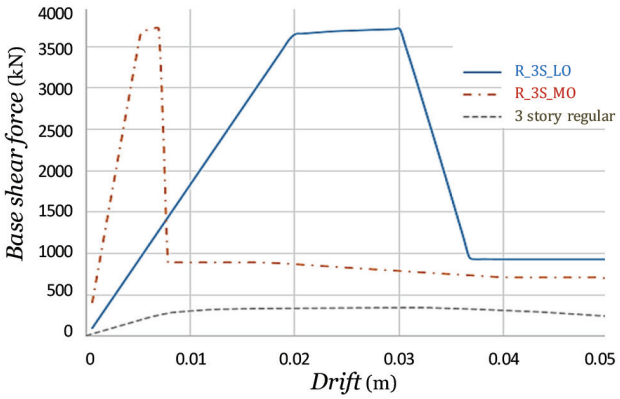

Fig. 13 The pushover curves of structures created by wall placement in the regular 3-story structure

(Eads, "Openseewiki"). Based on the curve in Fig. 13, the R_3S_MO structure has reached the maximum shear force in less drift compared to the R_3S_LO structure. It can be seen in Fig. 13 that the amount of base shear has increased significantly with the placement of the shear wall in a regular 3-story structure. Due to the fact that the behavior of the structures is not fully determined by applying drift at the roof point, here more drift is employed. Fig. 14 illustrations the pushover curves of structures created by wall placement in the irregular 3-story structure. Here the pushover curves continue to drift at the roof point. The behavior of IR_3S_MO and IR_3S_RO structures is flexural behavior. So, the decay occurs in them, and the shear wall application has less effect on them. According to Figs. 13 and 14, when the behavior of the thick shear wall dominates the behavior of structures, a sharp drop in the behavior curve occurs. The curve then decreases to the residual value of the structural strength and continues in that area. The pushover curves of structures created by wall placement in the regular 8-story structure are revealed in Fig. 15. The diagram continues to drift at the roof point. In increasing the amount of base shear force, the effect of shear wall placement on the frames is clearly evident.

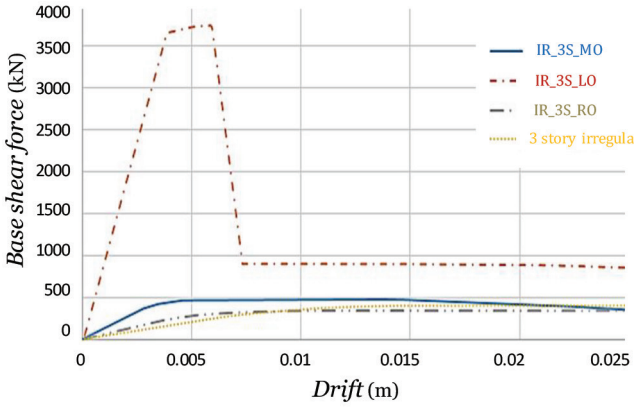

Fig. 14 The pushover curves of structures created by wall placement in the irregular 3-story structure

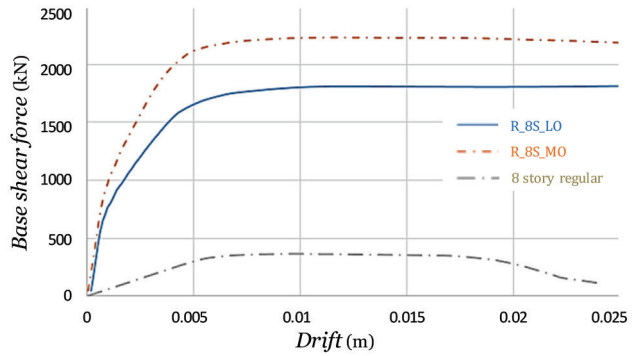

Fig. 15 The pushover curves of structures created by wall placement in the regular 8-story structure

Fig. 15 indications that the R_8S_MO structure has more capacity than the R_8S_LO structure. As a result, when the thin shear wall is placed in the middle opening of the regular 8-story structure, it creates more capacity than when the wall is in the side opening of the structure. The pushover curves of structures created by wall placement in the irregular 8-story structure are also presented in Fig. 16. It is clear that the IR_8S_LO structure has the highest base shear force. This is due to the difference in wall height in the structures. Also, the behavior of the shear wall dominates the behavior of the structure in this model.

The IR_8S_MO and IR_8S_RO structures decay faster than the walless structure, and their decline has begun in the drift. But for the IR_8S_LO structure, the decline starts approximately from the drift.

5 Applied earthquake and performance levels

Christchurch earthquake records with a magnitude of 7.1 (in the Canterbury region) and the related aftershocks by the end of 2011 are considered. In this research, the applied records have a PGA of more than 0.05g in 3 directions [11]. To generate seismic sequences, there are only 15 acceptable stations to use their data (see Table 6). Also, the rest time between each record is set at 5 seconds to create a seismic sequence. After sequencing the main earthquakes and aftershocks from 15 earthquake stations, the 15 seismic sequences are obtained. The original earthquake records of the 2010 New Zealand Christchurch earthquake and related aftershocks by the end of 2011 can be downloaded from "*the GeoNet processed strong-motion data site*". For instance, only a few accelerometers of the original earthquake records and seismic sequences are mentioned (Figs. 17 and 18).

For the IDA analysis by spectral acceleration method, it is necessary to first acquire the spectrum of these sequences with a damping ratio of 0.05 and the number corresponding

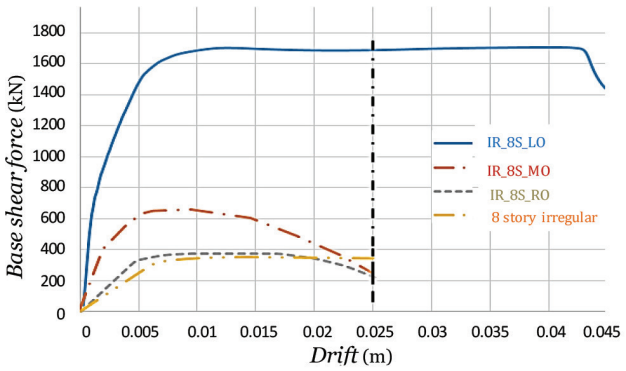

Fig. 16 The pushover curves of structures created by wall placement in the irregular 8-story structure

Table 6 The station names and the number of corresponding records

No.	Station name	Abbreviation	Sequences
1	Christchurch Canterbury Aero Club	CACS	3
2	Christchurch Botanic Gardens	CBGS	8
3	Christchurch Cathedral College	CCCC	5
4	Christchurch Cashmere High School	CMHS	12
5	Canterbury Ring Laser	CRLZ	6
6	Darfield High School	DFHS	4
7	Heathcote Valley Primary School	HVSC	16
8	Lincoln Crop and Food Research	LINC	11
9	Christchurch North New Brighton School	NNBS	4
10	Christchurch Papanui High School	PPHS	4
11	Pages Road Pumping Station	PRPC	25
12	Christchurch Resthaven	REHS	7
13	Riccarton High School	RHSC	6
14	Shirley Library	SHLC	5
15	Swannanoa School	SWNC	2

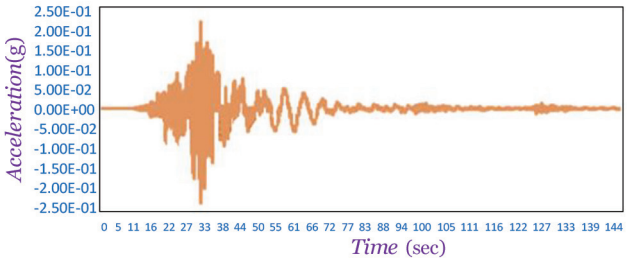

Fig. 17 Horizontal component of the main earthquake of CACS station in N50W direction

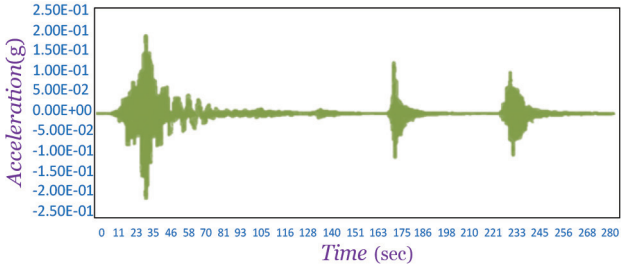

Fig. 18 Horizontal component of the seismic sequence of CACS station in N50W direction

Table 7 The seismic hazard zones related to UBC regulations

Zone	1	2A	2B	3	4
Acceleration (g)	0.075	0.15	0.20	0.30	0.40

to the period of the first mode of each structure in the spectrum of these records is determined. In during the analysis process, this number ($\sqrt[2]{S_{A1} \times S_{A2}}$) is then applied to the denominator of the corresponding record scale ($S_{A1,2}$ = Spectral acceleration of horizontal directions).

In this study, MATLAB software is applied to calculate the spectrum of records. To stop the IDA analysis operation, the collapse points based on performance levels have been introduced. For this purpose, the Hazus code has been utilized in this research.

As mentioned, the main frames of the present study are designed based on the acceleration of 0.2 ground acceleration. This amount of acceleration in the European regulations is part of the high seismic hazard zone. However, according to the Hazus Code, which is based on the UBC Code, this amount of acceleration is within the moderate seismic hazard zone. The seismic hazard zones related to UBC regulations are presented in Table 7. Given that the acceleration of the design basis is 0.2g, then zone 2B is selected and performance levels appropriate to this zone are considered. Table 8 are performance levels derived from the Hazus code. In this research, the average drift of performance levels of flexural frame and shear wall will be employed. Table 8 illustrations these collapse drifts.

After determining the collapse acceleration, a series of points are gained based on the performance levels. So, fragility curves are considered to represent these points. In these curves, the vertical axis indicates the probability of failure, and the horizontal axis denotes the acceleration of collapse of the structure under the imposed records. The fragility curves are created to estimate the failure potential of structures under earthquakes. The Eq. (1) is utilized to calculate the probability of failure in these diagrams:

Table 8 Performance levels used for fragility curves and building collapse

Building type	Drift floors on the verge of failure			
	Slight	Moderate	Extensive	Complete
Regular and irregular 3-story flexural concrete frames	0.005	0.0087	0.0233	0.06
Regular and irregular 8-story flexural concrete frames	0.0025	0.0043	0.0117	0.03
Regular and irregular 3-story flexural concrete frames along with the shear wall	0.0045	0.00855	0.02325	0.06
Regular and irregular 8-story flexural concrete frames along with the shear wall	0.00225	0.00425	0.01165	0.03

$$P(X) = \Phi\left[(\ln X - \mu)/\sigma\right]. \quad (1)$$

Here Φ[] stands for the normal distribution function. Also σ represents the standard deviation and μ is the mean.

Excel software has been employed to acquire the acceleration points of collapse against the probability of occurrence. The best polynomial diagram are applied to fit between the points.

6 Results and discussion

6.1 Results of IDA analysis

After performing the pushover analysis and presenting the results of this analysis, the IDA analysis is performed on the considered structures. The responses of these structures at the mentioned levels are displayed as the fragility curves due to the failure of structures in 4 levels under main earthquake and seismic sequences.

6.1.1 IDA analysis for the regular 3-storey models with shear walls

The results of the developed structures are now presented so that the location of the shear wall in their openings has changed. On the first floor of 3-story structures, shear rupture occurs because the behavior of the thick wall governs the overall behavior of the structure. The regular 3-storey models along the wall under main earthquakes are evaluated in the IDA analysis. Their fragility curves are given in Fig. 19.

Due to the convergence of the Extensive and Complete performances, only the Extensive performance is considered. Fig. 19 displays that applying the shear wall in the middle opening of the regular 3-story structure can increase the likelihood of failure.

In the fragility curves, the word "poly" stands for Polynomial, which refers to the type of diagram used. The results of spectral acceleration (in the form of median) are now displayed at the mentioned performance levels. Fig. 20 also indications that the median spectral accelerations of the R_3S_LO structure are greater than the R_3S_MO structure. It can be said that in the almost three levels of performance, the proportions of differences are within the same range.

After the results of regular 3-story structures with shear walls under main earthquakes are stated, the results of these structures are now listed under seismic sequences. For this case, the median spectral acceleration of the data for each model is mentioned in the three performance levels. Figs. 21 and 22 also show that the failure probability of the R_3S_MO structure are greater than the R_3S_LO

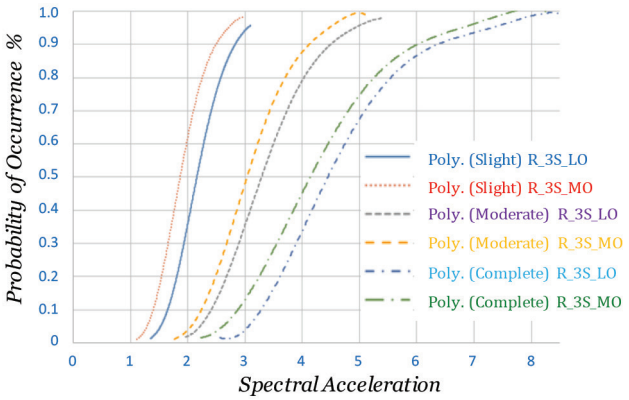

Fig. 19 Fragility curves of the R_3S_LO and R_3S_MO structures under main earthquakes

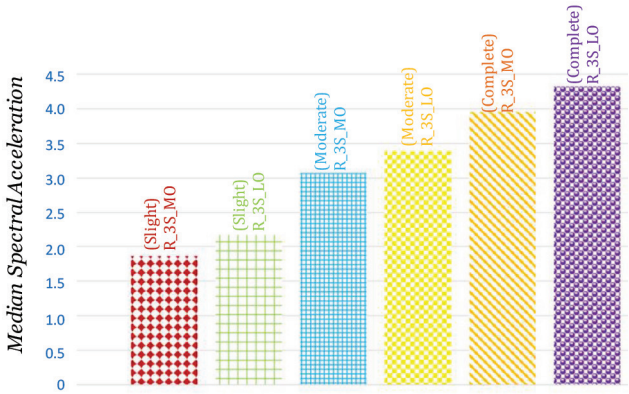

Fig. 20 Median spectral acceleration of the R_3S_LO and R_3S_MO structures under main earthquakes

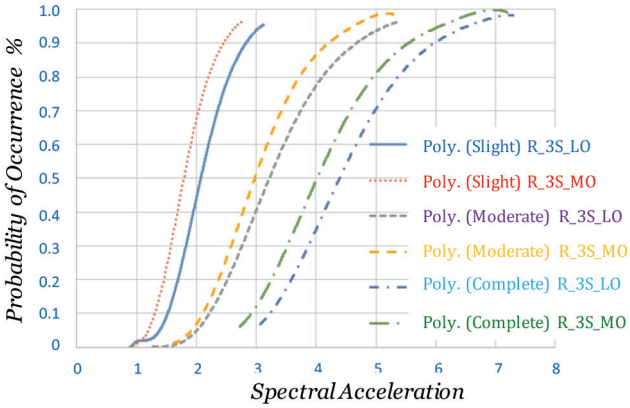

Fig. 21 Fragility curves of the R_3S_LO and R_3S_MO structures under seismic sequences

structure (at the same spectral acceleration). The R_3S_MO structure undergoes more spectral acceleration than other structures until a failure occurs. So, the result of Fig. 22 is inconsistent with Fig. 20.

Now, to justify this difference, both structures are compared for the same spectral accelerations created by a record, so that the results clarify the difference between the results mentioned in this section.

The spectral acceleration of 4.2 corresponding to the Complete level and another 1.45 related to the Slight level are selected for analysis. The results of this analysis are presented in Fig. 23. The results of Fig. 23 show that for each of the spectral accelerations, the R_3S_LO structure has a lower drift and lower base shear force than the R_3S_MO structure.

6.1.2 IDA analysis for the regular 8-storey models with shear walls

Initially, the fragility curves of these structures are displayed under main earthquakes. According to the displayed curves (Fig. 24), it seems that the application of a thin wall in the middle of the regular 8-story structures has a positive effect and as a result, a safer structure is created. At the Slight level, it can be seen that some records in two structures have almost the same intensities to produce the same failure (drift), and others require more spectral acceleration for the same drift. Thus, more spectral acceleration is required for the failure of R_8S_MO structure.

The median results of the spectral acceleration of these structures under applied loads are similar to previous results. It is worth noting that a number of figures are not presented in this section due to their similarity and to avoid crowding the article. After obtaining the results of main earthquakes, the results of applying seismic sequences are now expressed as the fragility curves and the median of spectral acceleration results.

According to Fig. 25, the closeness of some fragility diagrams is due to the fact that a series of spectral acceleration intensities of records for the two structures are close to each other (at some performance levels). Here, the studied 8-storey structures are exposed to main earthquakes and seismic sequences, and the probability of structural failure due to main earthquakes and seismic sequences with the same spectral acceleration is investigated.

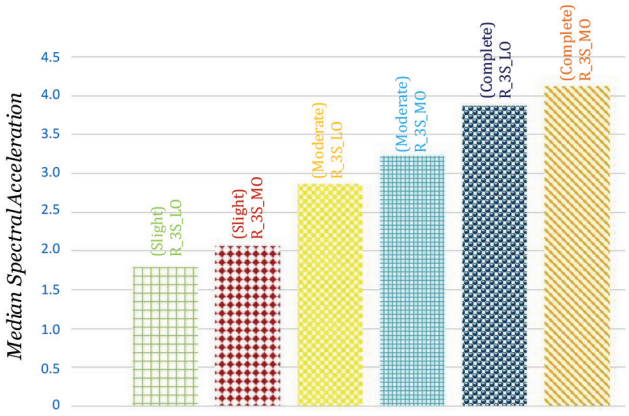

Fig. 22 Median spectral acceleration of the R_3S_LO and R_3S_MO structures under seismic sequences

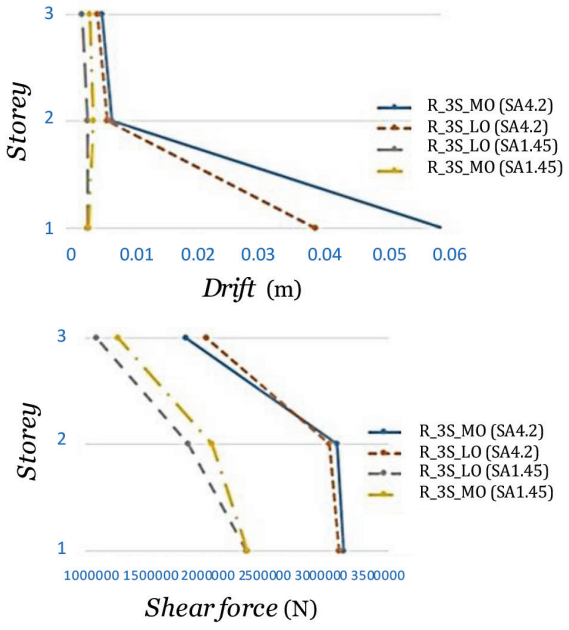

Fig. 23 Analysis results of the R_3S_LO and R_3S_MO structures under spectral accelerations of 1.45 and 4.2

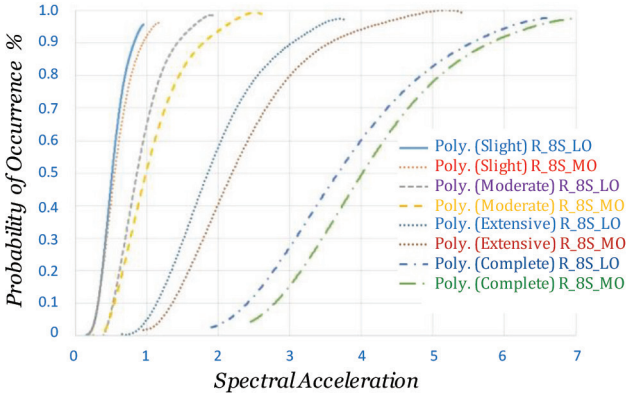

Fig. 24 Fragility curves of the R_8S_LO and R_8S_MO structures under main earthquakes

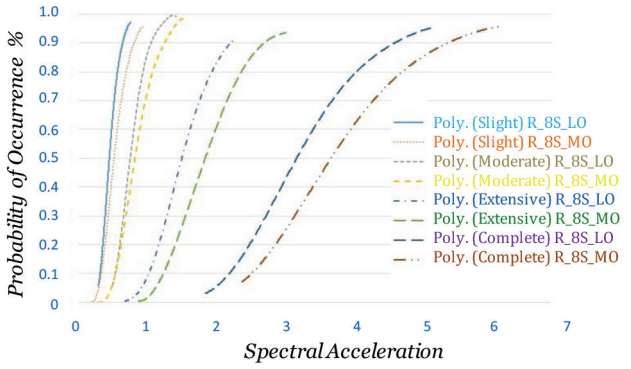

Fig. 25 Fragility curves of the R_8S_LO and R_8S_MO structures under seismic sequences

Hereof, Figs. 26 and 27 represent the results of this analysis for R_8S_LO and R_8S_MO structures. Based on the results, it can be said that for the same spectral acceleration in two cases, more damage occurs due to the application of seismic sequences because the applied aftershocks cause these failures. The R_8S_LO and R_8S_MO structures are now compared under a specific record. In Fig. 28, the structures are subjected to the same spectral acceleration. According to the written code for IDA analysis, the analysis operation stops when the R_8S_LO structure reaches the target drift (0.03 m). The R_8S_LO structure has reached the target drift in approximately 30 seconds and the analysis operation is stopped. However, the R_8S_MO structure did not reach the final drift at this spectral acceleration, so the analysis was performed until the end of the record. Therefore, it is concluded that the R_8S_MO structure has more strength and better performance than the R_8S_LO structure. In addition, Fig. 29 confirms this conclusion.

6.1.3 IDA analysis for the irregular 3-storey models with shear walls

In the next step, the results of irregular structures are evaluated. According to the results obtained from the research of Hosseinpour and Abdolnabi [11], the application of vertical acceleration in the seismic analysis has no significant effect on the regular structures. Therefore, the vertical acceleration component is applied only to the irregular structures. In this type of structures, the normalization coefficients have been utilized in the main earthquake application section. The method of obtaining these coefficients was mentioned in the FEMA P695 report [32]. The reason for considering this method is that the intensity of the records is distributed proportionally and there is less intensity concentration in the curve. In this way, the obtained coefficients are multiplied in the scale coefficient of applied earthquake and may increase or decrease the intensity of the applied earthquake. Figs. 30 and 31 show that applying the vertical acceleration of the main earthquakes to the IR_3S_LO and IR_3S_MO structures does not have much effect on the performance levels (with respect to the case where the vertical acceleration is not applied.). Also in Fig. 32, the performance levels of the IR_3S_RO structure are presented under the application of horizontal components and under the application of horizontal + vertical components of main earthquakes. With and without applying the vertical acceleration, it can be said that the fragility curves of the IR_3S_RO structure are slightly different in the four performance levels (see Fig. 32).

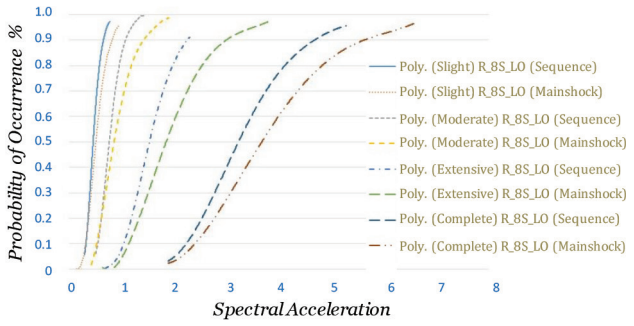

Fig. 26 Fragility curves of the R_8S_LO structures under main earthquakes and seismic sequences

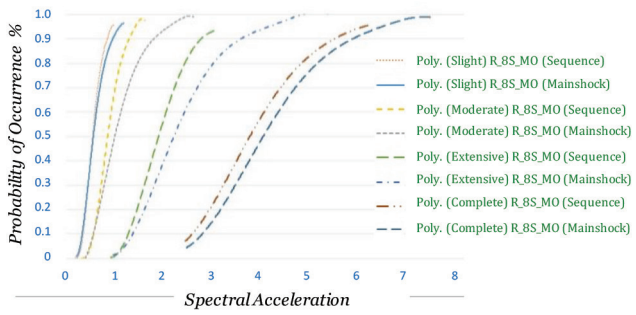

Fig. 27 Fragility curves of the R_8S_MO structures under main earthquakes and seismic sequences

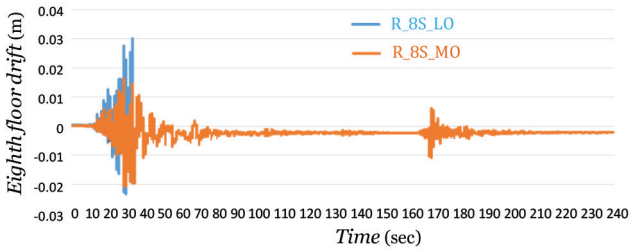

Fig. 28 Comparison of drift history of the R_8S_LO and R_8S_MO structures under spectral acceleration of 4.5

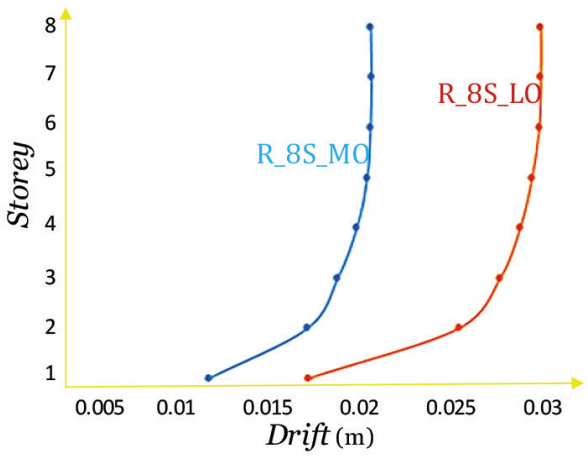

Fig. 29 Drift of the floors of the R_8S_LO structure under spectral acceleration of 4.5

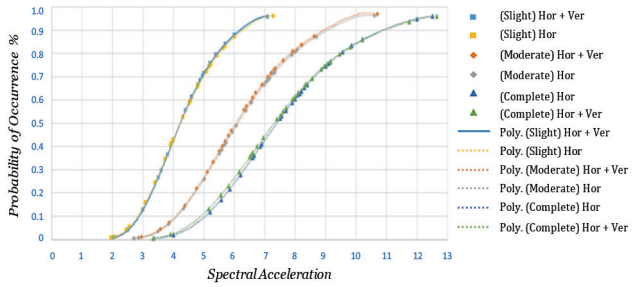

Fig. 30 Fragility curve of the IR_3S_LO structure by applying horizontal components and by applying horizontal + vertical components of main earthquakes

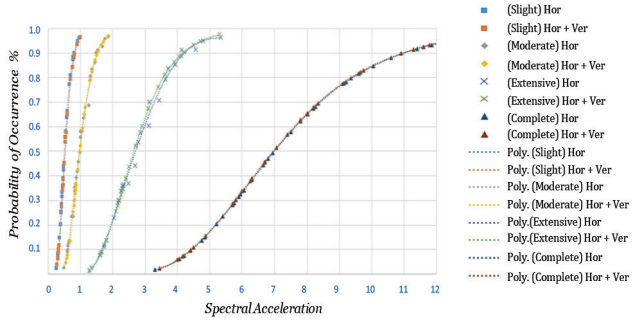

Fig. 31 Fragility curve of the IR_3S_MO structure by applying horizontal components and by applying horizontal + vertical components of main earthquakes

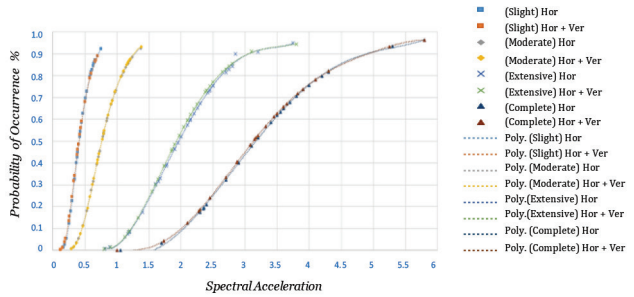

Fig. 32 Fragility curve of the IR_3S_RO structure by applying horizontal components and by applying horizontal + vertical components of main earthquakes

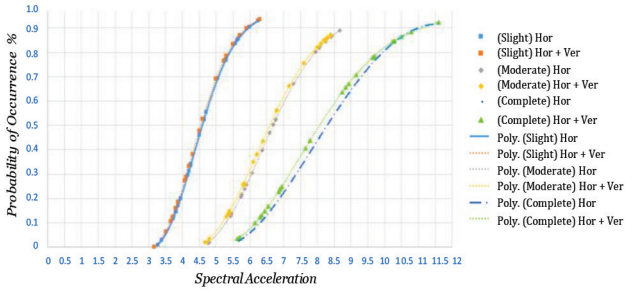

Fig. 33 Fragility curve of the IR_3S_LO structure by applying horizontal components and by applying horizontal + vertical components of seismic sequences

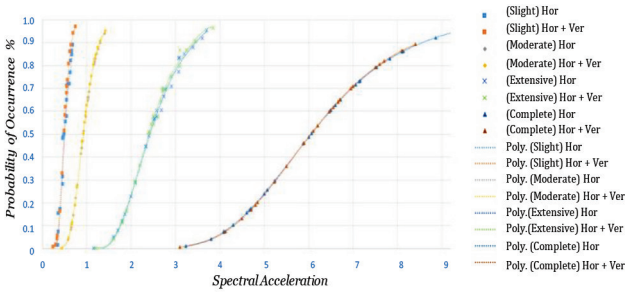

Fig. 34 Fragility curve of the IR_3S_MO structure by applying horizontal components and by applying horizontal + vertical components of seismic sequences

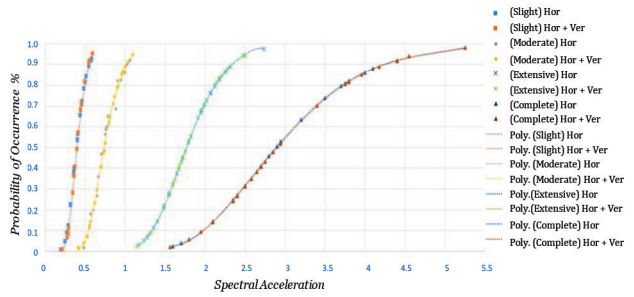

Fig. 35 Fragility curve of the IR_3S_RO structure by applying horizontal components and by applying horizontal + vertical components of seismic sequences

Also, the obtained results show that the median spectral acceleration of irregular 3-story structures (with shear wall) under main earthquakes with and without applying the vertical acceleration are not significantly different for a similar failure rate, and the maximum difference is about 1 to 2.5%.

These structures are now analyzed under seismic sequences with and without applying vertical acceleration. Based on the results presented in Fig. 33, Slight and Moderate levels did not change. But at the Complete level, there is a slight difference if vertical acceleration is applied.

However, this difference is about 2.5%. According to Figs. 34 and 35, applying vertical acceleration of seismic sequences to IR_3S_MO and IR_3S_RO structures have no significant effect on the four performance levels. For better conclusions, the median spectral accelerations for these structures are now expressed at different performance levels. The obtained results display that the median spectral acceleration for each structure at different performance levels does not change significantly when the vertical acceleration is applied. The largest change between the two cases at the Moderate level is related to the IR_3S_LO structure, although this difference is about 2.5%. Therefore, the vertical acceleration component of the earthquake does not have a significant effect on these structures.

6.1.4 IDA analysis for the irregular 8-storey models with shear walls

The normalization coefficients have been employed for these structures in the application of main earthquakes. The reasons for utilizing these coefficients are stated in the previous section. In this section, the three irregular 8-story structures with shear walls under main earthquakes are compared separately with applying the horizontal acceleration as well as horizontal acceleration + vertical acceleration. Figs. 36, 37 and 38 represent that there is the greatest effect of the vertical acceleration of the main earthquakes in the IR_8S_LO structure that the behavior of thin wall dominates the behavior of the structure.

This effect is clearly evident in the four levels of performance. In the other two structures, the effect of vertical acceleration on the four performance levels is negligible. As expected, the median spectral acceleration in IR_8S_MO and IR_8S_RO structures under vertical acceleration did not change significantly. So, in these structures, the vertical acceleration caused by the main earthquakes has the greatest influence on the IR_8S_LO structure and this effect is significant. In addition, the three irregular 8-story structures with shear walls under the seismic sequences are compared separately with applying the horizontal acceleration as well as horizontal acceleration + vertical acceleration. The overall results are quite similar to the previous case.

The IR_8S_LO structure will be analyzed under the spectral acceleration of 3.3 resulting from an earthquake with and without vertical acceleration, and its results will be displayed for better evaluation.

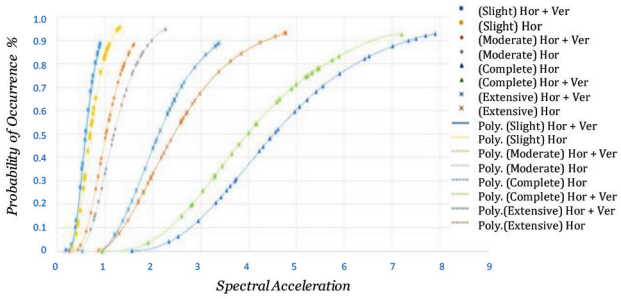

Fig. 36 Fragility curve of the IR_8S_LO structure by applying horizontal components and by applying horizontal + vertical components of main earthquakes

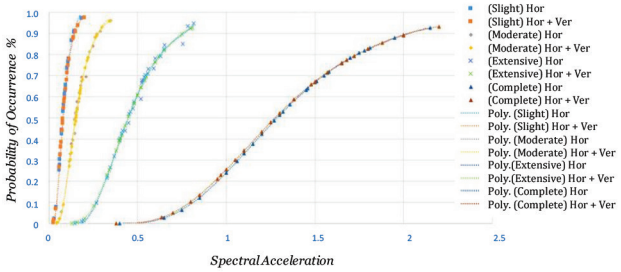

Fig. 37 Fragility curve of the IR_8S_MO structure by applying horizontal components and by applying horizontal + vertical components of main earthquakes

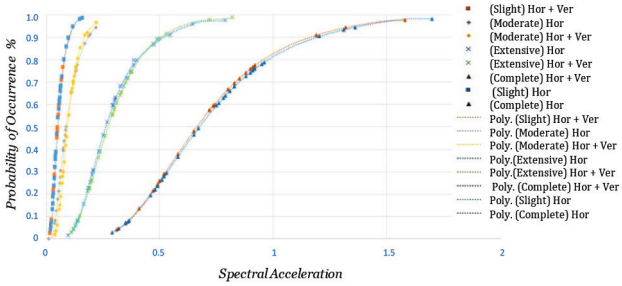

Fig. 38 Fragility curve of the IR_8S_RO structure by applying horizontal components and by applying horizontal + vertical components of main earthquakes

7 Conclusions

Generally, the time spans between seismic sequences are short and there is not enough time to retrofit the structures of buildings against subsequent earthquakes. Accordingly, the stiffness and strength of the building are reduced due to the occurrence of possible damages. Therefore, the aim of the present study is to investigate the location of shear walls in the regular and irregular 3- and 8-story structures under main earthquakes and seismic sequences using IDA analysis. In other words, the shear walls are located in the openings of regular and irregular 3- and 8-story structures according to the created characteristics (thick or thin) and are analyzed under Christchurch earthquake and corresponding seismic sequences utilizing IDA analysis. The results of these analyzes are presented in the form of fragility curves and the median spectral accelerations. In extracting the results, the failure index is considered as the maximum drift between the floors of the structures. The results are summarized as follows:

- In the case of the thick shear wall located in the middle of the regular 3-story reinforced concrete structures (R_3S_MO), there is a high probability of failure. The difference in the median spectral acceleration of the two structures R_3S_MO and R_3S_LO at the three performance levels (Slight, Moderate, Complete) for the main earthquakes are approximately 13%, 11%, and 11%, respectively, and for the seismic sequences are approximately 15%, 12%, and 6%.
- Under all records of earthquakes with the same spectral acceleration, the damage caused to the R_3S_MO structure is greater than the R_3S_LO structure.

- With the placement of the thick wall in the middle opening of the regular 3-story reinforced concrete frame, the median value of spectral acceleration under seismic sequences at the three performance levels (Slight, Moderate, Complete) increased 11, 12 and 3 times, respectively.
- In the case of the thin shear wall located in the middle opening of the regular 8-story reinforced concrete structures (R_8S_MO), the probability of failure is low (when the spectral accelerations are approximately higher than 0.7g).
- The difference in the damage reduction between the R_8S_MO and R_8S_LO structures will gradually increase at higher intensities and the R_8S_MO structure will be more durable.
- The difference in the median spectral acceleration of the two structures R_8S_MO and R_8S_LO at the four performance levels (Slight, Moderate, Extensive, Complete) for the main earthquakes are approximately equal, 20%, 18% and almost equal and under seismic sequences are approximately 22%, 17%, 24%, 16%, respectively.
- Applying the vertical acceleration related to the main earthquakes or seismic sequences in the irregular 3-story reinforced concrete structures, there is no significant change in the fragility curve.
- The IR_3S_MO structure under main earthquakes at the three performance levels (Slight, Moderate, Complete) can withstand 11%, 14% and 88% spectral acceleration more than the IR_3S_LO structure, respectively. This ratio is approximately 10%, 12% and 42% for the IR_3S_RO structure, respectively.
- In the fragility curves obtained for irregular 8-story reinforced concrete structures with shear wall, the vertical acceleration has the greatest effect on the IR_8S_LO structure.
- In the IR_8S_LO structure, the concrete and longitudinal rebars of shear wall in higher floors are subjected to more stress if vertical acceleration is applied.

References

[1] Song, R., Li, Y., Van de Lindt, J. W. "Loss estimation of steel buildings to earthquake mainshock-aftershock sequences", Structural Safety, 61, pp. 1–11, 2016. https://doi.org/10.1016/j.strusafe.2016.03.002

[2] Shafaei, H., Naderpour, H. "Seismic fragility evaluation of FRP-retrofitted RC frames subjected to mainshock-aftershock records", Structures, 27, pp. 950–961, 2020. https://doi.org/10.1016/j.istruc.2020.07.018

[3] Amadio, C., Fragiacomo, M., Rajgelj, S. "The effects of repeated earthquake ground motions on the non-linear response of SDOF systems", Earthquake Engineering & Structural Dynamics, 32(2), pp. 291–308, 2003. https://doi.org/10.1002/eqe.225

[4] Hatzigeorgiou, G. D., Liolios, L. L. "Nonlinear behaviour of RC frames under repeated strong ground motions", Soil Dynamics and Earthquake Engineering, 30, pp. 1010–1025, 2010 https://doi.org/10.1016/j.soildyn.2010.04.013

[5] Abdelnaby, A. E., Elnashai, A. S. "Performance of degrading reinforced concrete frame systems under the Tohoku and Christchurch earthquake sequences", Journal of Earthquake Engineering, 18(7), pp. 1009–1036, 2014. https://doi.org/10.1080/13632469.2014.923796

[6] Moshref, A., Tehranizadeh, M., Khanmohammadi, M. "Investigation of the reliability of nonlinear modeling approaches to capture the residual displacements of RC columns under seismic loading", Bulletin of Earthquake Engineering, 13, pp. 2327–2345, 2015. https://doi.org/10.1007/s10518-014-9718-6

[7] Abdelnaby, A. E., Elnashai, A. S. "Numerical modeling and analysis of RC frames subjected to multiple", Earthquakes and Structures, 9(5), pp. 957–981, 2015. https://doi.org/10.12989/eas.2015.9.5.957

[8] Abdelnaby, A. E. "Fragility curves for RC frames subjected to Tohoku mainshock-aftershocks sequences", Journal of Earthquake Engineering, 22(5), pp. 902–920, 2018. https://doi.org/10.1080/13632469.2016.1264328

[9] Wen, W., Zhai, C., Ji, D., Li, S., Xie, L. "Framework for the vulnerability assessment of structure under mainshock-aftershock sequences", Soil Dynamics and Earthquake Engineering, 101, pp. 41–52, 2017. https://doi.org/10.1016/j.soildyn.2017.07.002

[10] Hosseinpour, F., Abdelnaby, A. E. "Fragility curves for RC frames under multiple earthquakes", Soil Dynamics and Earthquake Engineering, 98, pp. 222–234, 2017. https://doi.org/10.1016/j.soildyn.2017.04.013

[11] Hosseinpour, F., Abdelnaby, A. E. "Effect of different aspects of multiple earthquakes on the nonlinear behavior", Soil Dynamics and Earthquake Engineering, 92, pp. 706–725, 2017. https://doi.org/10.1016/j.soildyn.2016.11.006

[12] Rostamian, M., Hosseinpour, F., Abdelnaby, A. E. "Effect of seismic retrofitting on the behavior of RC bridge columns subjected", presented at Structures Congress 2017, Denver, USA, April 6–8, 2017. https://doi.org/10.1061/9780784480403.038

[13] Omranian, E., Abdelnaby, A. E., Abdollahzadeh, G. H., Rostamian, M., Hosseinpour, F. "Fragility curve development for the seismic vulnerability assessment of retrofitted RC bridges under mainshock-aftershock seismic sequences", presented at Structures Congress 2018, Fort Worth, TX, USA, April 19–21, 2018. https://doi.org/10.1061/9780784481332.028

[14] Moradiyan, M., Pachideh, G., Moshtagh, A. "Study of seismic behavior and development of fragility curves of divergent braced frames under successive earthquakes", Journal of Structural and Construction Engineering, 8(4), pp. 156–175, 2022. https://doi.org/10.22065/JSCE.2021.263292.2315

[15] Kheyroddin, A., Gholhaki, M., Pachideh, G. "Seismic evaluation of reinforced concrete moment frames retrofitted with steel braces using IDA and pushover methods in the near-fault field", Journal of Rehabilitation in Civil Engineering, 7(1), pp. 159–173, 2019. https://doi.org/10.22075/JRCE.2018.12347.1211

[16] Yadegari, A., Pachideh, G., Gholhaki, M., Shiri M. "Seismic Performance of C-PSW", In: 2nd International Conference on Civil Engineering, Architecture and Urban Planning Elites, London, England, 2016, pp. 110–123.

[17] Oyguc, R., Toros, C., Abdelnaby, A. E. "Seismic behavior of irregular reinforced-concrete structures under multiple", Soil Dynamics and Earthquake Engineering, 104, pp. 15–32, 2018. https://doi.org/10.1016/j.soildyn.2017.10.002

[18] Hamidi Jamnani, H., Vaseghi Amiri, J., Rajabnejad, H. "Energy distribution in RC shear wall-frame structures subject to repeated earthquakes", Soil Dynamics and Earthquake Engineering, 107, pp. 116–128, 2018. https://doi.org/10.1016/j.soildyn.2018.01.010

[19] Amiri, S., Bojórquez, E. "Residual displacement ratios of structures under mainshock-aftershock sequences", Soil Dynamics and Earthquake Engineering, 121, pp. 179–193, 2019. https://doi.org/10.1016/j.soildyn.2019.03.021

[20] Hassan, E. M., Admuthe, S., Mahmoud, H. "Response of semi-rigid steel frames to sequential earthquakes", Journal of Constructional Steel Research, 173, 106272, 2020. https://doi.org/10.1016/j.jcsr.2020.106272

[21] Di Sarno, L., Wu, J.-R. "Fragility assessment of existing low-rise steel moment-resisting frames with masonry infills under mainshock-aftershock earthquake sequence", Bulletin of Earthquake Engineering, 19, pp. 2483–2504, 2021. https://doi.org/10.1007/s10518-021-01080-6

[22] FEMA "HAZUS-MH MR4 Technical Manual, Earthquake Model", Federal Emergency Management Agency, Washington, DC, USA, 2003.

[23] BSI "Eurocode 8: Design of Structures for Earthquake Resistance, Part 1: General rules, Seismic actions and rules for buildings", European Committee for Standardization, Brussels, Belgium, 2005.

[24] Haselton, C. B., Liel, A. B., Lange, S. T., Deierlein, G. G. "Beam-column element model calibrated for predicting flexural response leading to global collapse of RC frame buildings", Pacific Earthquake Engineering Research Center, Berkeley, CA, USA, Rep. 2007/03, 2008.

[25] Ibarra, L. F., Krawinkler, H. "Global collapse of frame structures under seismic excitations", Pacific Earthquake Engineering Research Center, Stanford, CA, USA, Rep. 152, 2005.

[26] Telemachos, B., Fardis, N. M. "Deformations of reinforced concrete members at yielding and ultimate", ACI Structural, 98(2), pp. 135–148, 2001. https://doi.org/10.14359/10181

[27] ACI 318-14. Building Code Requirements for Structural Concrete, American Concrete Institute, Farmington Hills, MI, USA, 2014.

[28] Elwood, K. J., Matamoros, A. B., Wallace, J. W., Lehman, D., Heintz, J. A., …., Moehle, J. P. "Update to ASCE/SEI 41 concrete provisions", Earthquake Spectra, 23(3), pp. 493–523, 2007. https://doi.org/10.1193/1.2757714

[29] Kolozvari, K., Orakcal, K., Wallace, J. "Shear-flexure interaction modeling for reinforced concrete structural walls and columns under reversed cyclic loading", Pacific Earthquake Engineering Research Center Headquarters at the University of California, Berkeley, CA, USA, Rep. 2015/12, 2015.

[30] Orakcal, K., Wallace, J. W., Conte, J. P. "Flexural modeling of reinforced concrete structural walls - Model Attributes", ACI Structural Journal, 101(5), pp. 688–698, 2004. https://doi.org/10.14359/13391

[31] ASCE 7-10: American Society of Civil Engineers. Minimum design loads for buildings and other structures, American Society of Civil Engineers, Reston, VA, USA, 2013. https://doi.org/10.1061/9780784412916

[32] FEMA P695 Applied Technology, Council, "Quantification of building seismic performance factors", Federal Emergency Management Agency, Washington, DC, USA, 2008.